4

AMORPHOUS AZOBENZENE POLYMERS FOR LIGHT-INDUCED SURFACE PATTERNING

Kevin G. Yager and Christopher J. Barrett

4.1. SURFACE MASS TRANSPORT

In 1995, a surprising and unprecedented optical effect was discovered in polymer thin films containing the azo chromophore Disperse Red 1 (DR1), shown in Fig. 4.1. The Natansohn/Rochon (Rochon et al., 1995) research team and the Tripathy/Kumar collaboration (Kim et al., 1995b) simultaneously and independently discovered a large-scale surface mass transport when the films were irradiated with a light interference pattern. In a typical experiment, two coherent laser beams, with a wavelength in the azo absorption band, are intersected at the sample surface (Fig. 4.2a, b). The sample usually consists of a thin spin-cast film (10–1000 nm) of an amorphous azopolymer on a transparent substrate. The sinusoidal light interference pattern at the sample surface leads to a sinusoidal surface patterning, that is, a surface relief grating (SRG). These gratings were found to be extremely large, up to hundreds of nanometers, as confirmed by atomic force microscopy (AFM) (Fig. 4.3). The SRGs diffract very efficiently, and in retrospect it is clear that many reports of large diffraction efficiency before 1995, attributed to birefringence, were in fact due to surface gratings. The process occurs readily at room temperature [well below the glass-to-rubber transition temperature (T_g) of the amorphous polymers used] with moderate irradiation (1–100 mW/cm^2) over seconds to minutes. The phenomenon is a reversible mass transport, not irreversible material ablation, since a flat film with the original thickness is recovered upon heating above T_g. Critically, it requires the presence and isomerization of azobenzene chromophores. Other absorbing but nonisomerizing chromophores do not produce SRGs. Many other systems can exhibit optical surface patterning (Yamaki et al., 2000), but the

Smart Light-Responsive Materials. Edited by Yue Zhao and Tomiki Ikeda

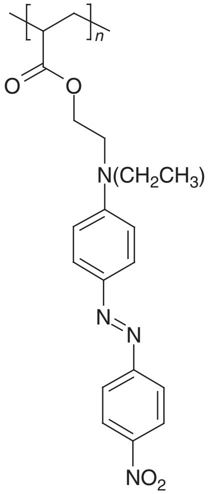

Figure 4.1. Chemical structure of poly(Disperse Red 1) acrylate, pdr1a, a pseudostilbene side-chain azopolymer that generates high quality surface relief structures.

amplitude of the modification is much smaller, does not involve mass transport, and usually requires additional processing steps. The all-optical patterning unique to azobenzenes has been studied intensively since its discovery, yet the mechanism remains controversial. The competing interpretations will be discussed and evaluated here. Many reviews of the remarkable body of experimental results are available (Natansohn and Rochon, 2002; Yager and Barrett, 2001; Delaire and Nakatani, 2000; Viswanathan et al., 1999b).

4.1.1. Experimental Observations

The surface mass patterning unique to azobenzenes is a fundamentally optical process, whereby the incident light pattern is encoded in the material. In an SRG experiment, two beams are intersected at an angle 2θ at the sample surface, giving rise to an SRG with period:

$$\Lambda = \frac{\lambda}{2\sin\theta} \tag{4.1}$$

where λ is the wavelength of the inscription light. The amplitude (height) of the SRG depends on the inscription angle, displaying a maximum at $\theta \sim 15^\circ$ (Barrett et al., 1996; Kim et al., 1995a). Grating height increases nonlinearly with irradiation time and power, up to a saturation point (Fukuda et al., 2000a; Bian et al., 1999). At moderate fluence, the grating efficiency depends only on the net exposure, not on the temporal distribution of irradiation. Gratings can be formed with intensities as low as $1\,\mathrm{mW/cm^2}$, as long as the inscription wavelength

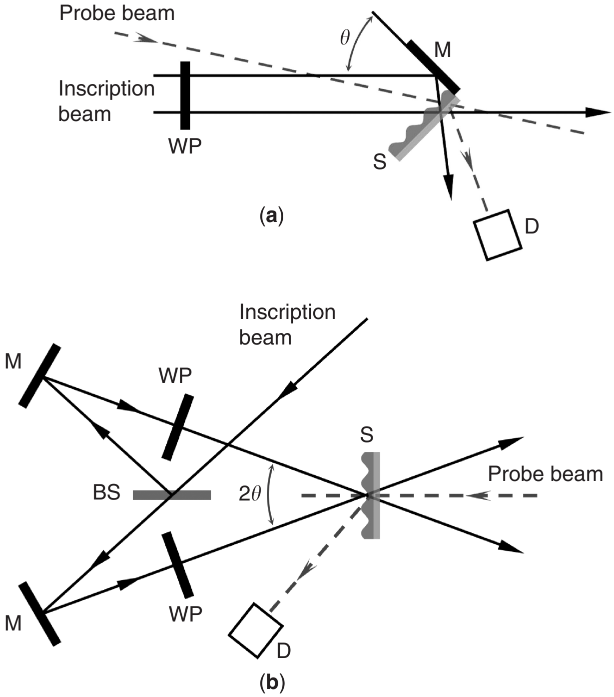

Figure 4.2. Experimental setup for the inscription of a surface relief grating: S refers to the sample, M are mirrors, D is a detector for the diffraction of the probe beam, WP is a waveplate (or generally a combination of polarizing elements), and BS is a 50% beam splitter. The probe beam is usually a HeNe (633 nm), and the inscription beam is chosen on the basis of the chromophore absorption band (often Ar^+ 488 nm). **(a)** A simple one-beam inscription involves reflecting half of the incident beam off of a mirror adjacent to the sample. **(b)** A two-beam interference setup enables independent manipulation of the polarization state of the two incident beams.

is within the azo absorption band. Most chromophores used for SRG formation have a strong overlap of their trans and cis absorption spectra, allowing both isomers to be excited with a single wavelength. However, some experiments have been performed using azobenzenes with trans absorption in the blue, and cis absorption in the red (Jager et al., 2001; Sanchez et al., 2000). Using an interference pattern of red HeNe beams, inscription only occurs if a blue pump beam concurrently irradiates. This biphotonic phenomenon proves that cycling of chromophores, and not simply isomerization, is required for grating formation.

The phase relationship between the incident light field and the resulting surface deformation is crucial in understanding the mechanism of grating formation (Fig. 4.4). Early investigations using the diffraction of an edge (Kumar et al.,

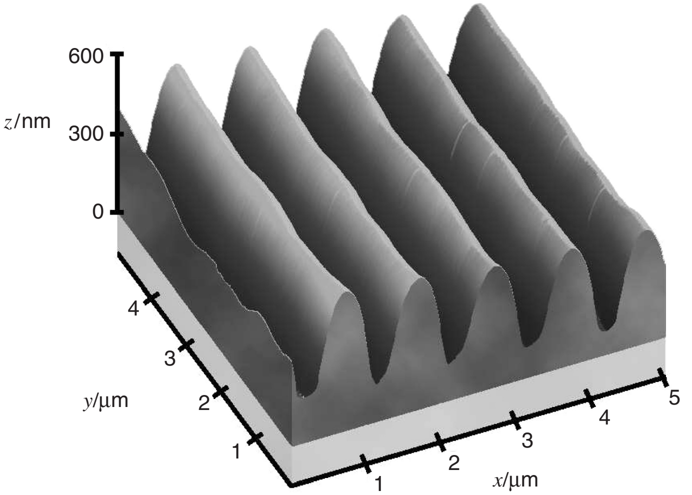

Figure 4.3. AFM image of a typical SRG optically inscribed into an azopolymer film. Grating amplitudes of hundreds of nanometers, on the order of the original film thickness, are easily obtained. In this image, the approximate location of the film-substrate interface has been set to $z = 0$ on the basis of knowledge of the film thickness.

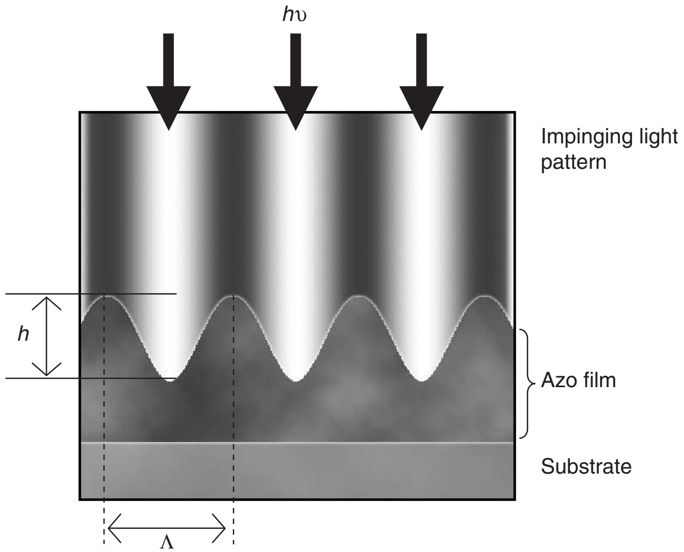

Figure 4.4. Schematic of a grating with spacing Λ and amplitude h. The usual phase relationship is indicated: light intensity maxima correspond to valleys in the surface relief.

1998; Kim et al., 1997; Rochon et al., 1995) and single-beam surface deformations (Bian et al., 1998) convincingly showed that the light and surface relief are 180° out of phase. In other words, light intensity maxima correspond to valleys in the surface relief. In effect, material is moved out of the light and into the dark regions. This rule appears to hold in the majority of cases, yet in a number of systems the phase relationship seems to be exactly inverted, with mass transport into illuminated regions. Specifically, in certain liquid crystalline (LC) systems, the phase behavior is inverted (Helgert et al., 2001; Bublitz et al., 2000; Holme et al., 1999). In one study, an amorphous material exhibited the "usual" phase behavior, and a thin film of this polymer floating on water expanded in the direction of the light polarization. A similar LC azopolymer exhibited inverted phase behavior in SRG experiments, and contracted in the direction of polarized illumination as a floating film. The tempting conclusion is that amorphous and polymeric systems exhibit opposite photomechanical response, which translates into opposite phase behavior in grating inscription. A possibly relevant experiment showed that for LC systems, the cis chromophores may become preferentially oriented along the light polarization direction, instead of being perpendicular to it (Hore et al., 2003). It should be pointed out, however, that some LC systems exhibit the usual phase relationship (Zettsu et al., 2003), and in one LC system, modification of a single ring substituent led to opposite phase behavior (Helgert et al., 2001).

Adding to the complexity of the phase relationship, it was observed that at high irradiation power ($>300\,\mathrm{W/cm^2}$), the behavior was inverted in amorphous systems (Bian et al., 1999). Single-beam experiments at high power showed a central peak instead of a depression. By exposing a sample to a gradient two-beam intersection, a film was inscribed with a continuum of laser intensitites. An in-phase grating was found in the high power region, and a conventional out-of-phase SRG was found in the low power region. The intermediate region clearly showed interdigitation of the peaks from the two regimes, resembling a doubling of grating period observed by others. These double-period gratings can be formed in a number of amorphous systems, using the polarization combinations of (p, p) or (+45°, −45°), with indications that even the (s, s) and (p, s) combinations function to a certain extent (Lagugne-Labarthet et al., 2004; Labarthet et al., 2001, 2000; Naydenova et al., 1998a). Observations of a double-frequency orientational grating underneath a normal SRG have also been reported (Schaller et al., 2003). The double-period SRGs were attributed to interference between the diffracted beams from the primary grating, which gives rise to a light modulation, with double the initial frequency, in the material. Whether these double-period gratings are related to the inverted structures observed in high intensity experiments and some LC systems is an open question. It is interesting to note that some of the amorphous polymers that exhibit double-frequency behavior have accessible LC phases at a higher temperature. These phase behavior results strongly suggest that there are (at least) two mechanisms at play during surface patterning. One dominates at low intensity in amorphous systems, whereas another appears to dominate at higher intensity and in LC systems. From an applied standpoint, these double-period gratings are of great interest, as they represent a means of generating patterned structures below the usual diffraction limit of far-field optical lithography.

The fact that the optical inscription process is sensitive to both intensity and polarization is of considerable importance (Jiang et al., 1996). Different polarization combinations lead to different amplitudes, *h*, of the inscribed SRG, as shown in Table 4.1. (The coordinate system is shown in Fig. 4.5.) An optical field vector component in the direction of light modulation (hence mass transport) appears necessary (Bian et al., 1998). Interestingly, SRGs can even be formed via pure polarization patterns, where the light intensity is uniform over the sample surface (Viswanathan et al., 1999a). In fact, the (*s*, *s*) and (RCP, RCP) combinations, which correspond to mainly variations in intensity and little to no polarization contrast, produce very poor SRGs. In contrast, the best gratings are obtained with (+45°, −45°) and (RCP, LCP) combinations, which involves primarily variation in polarization state across the film. It should be noted, however, that the exact polarization pattern present inside the material is not known. The pattern

TABLE 4.1. Polarization Patterns at the Sample Surface During SRG Inscription Using a Variety of Polarized Beam Combinations. The "Quality" of the SRG (as Determined by Grating Height) Is Shown for Comparison

Polarization of beams	Electric field in *xy* plane					SRG quality
x:	$+\pi$ $+\Lambda/2$	$+\pi/2$ $+\Lambda/4$	0 0	$-\pi/2$ $-\Lambda/4$	$-\pi$ $-\Lambda/2$	
s : s ↕ ↕	●	↕	↕	↕	●	6—Poor
s : p ↕ ↔	⤡	↺	⤢	↻	⤡	4
p : p ↔ ↔ *xy* Plane *xz* Plane	✶ ↕	↔ ↺	↔ ↔	↔ ↻	✶ ↕	3
+45° : +45° ⤢ ⤢	✶	⤢	⤢	⤢	✶	5
+45° : −45° ⤢ ⤡	↔	↺	↕	↻	↔	2—Good
RCP : RCP ↺ ↺	↺	↺	↺	↺	↺	7—Worst
RCP : LCP ↺ ↻	↔	⤢	↕	⤡	↔	1—Best

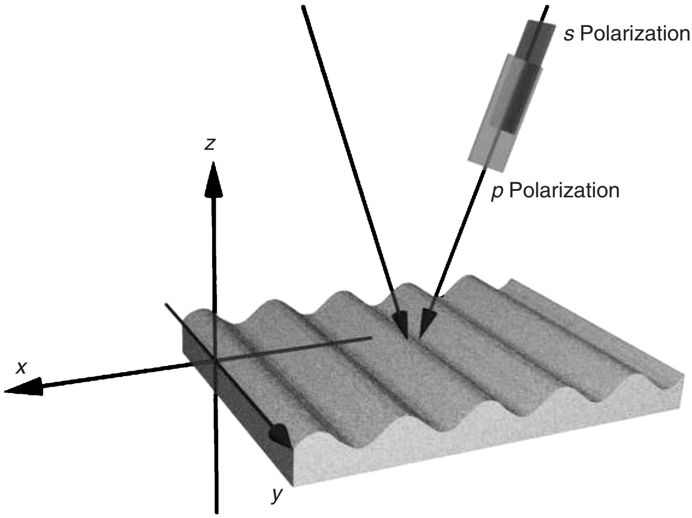

Figure 4.5. Coordinate system used to describe SRG inscription, with *x* running along the direction of light modulation. The two incident beams have their polarization state controlled. The *s* polarization is parallel to the surface, whereas the *p* state is parallel to the plane-of-incidence.

impinging on the sample is readily calculated from knowledge of the input polarizations, yet in the bulk of the material the light pattern will be redirected and repolarized on the basis of the detailed three-dimensional structure of the surface, refractive index, and birefringence. The optical erasure of an SRG, performed by homogenous irradiation, is also polarization-dependent (Lagugne-Labarthet et al., 2002; Jiang et al., 1998). Thus, the gratings possess a memory of the polarization state during inscription, encoded in the orientational distribution of chromophores at various grating positions. Typically, gratings inscribed with highly favorable polarization combinations will be optically erased more quickly. The *s*-polarization state, which produces poor gratings, is generally optimal for performing the erasure. These results are obviously related to the orientational distribution of chromophores after surface patterning and their subsequent interaction with the erasing polarization.

4.1.2. Patterning

In a typical inscription experiment, a sinusoidally varying light pattern is generated at the sample surface. What results is a sinusoidal surface profile: an SRG. This is the pattern most often reported in the literature, because it is conveniently generated (by intersecting two coherent beams) and easily monitored (by recording the diffraction intensity at a nonabsorbing wavelength, usually using a HeNe laser at 633 nm). However, it must be emphasized that the azo surface mass transport can produce arbitrary patterns. Essentially, the film encodes the impinging light pattern as a topography pattern. Both the intensity and polarization of light are encoded. What appears to be essential is a *gradient* in the intensity or polarization of the incident light field. For instance, a single focused gaussian laser spot will lead to a localized depression and a gaussian line will lead to an elongated trench. (Bian et al., 1998). In principle, any arbitrary pattern could be generated through an appropriate mask, interference/holographic setup, or scanning of a laser spot (Natansohn and Rochon, 2002).

Concomitant with the inscription of a surface relief is a photoorientation of the azo chromophores, which depends on the polarization of the incident beam(s). The orientation of chromophores in SRG experiments has been measured using polarized Raman confocal microspectrometry (Lagugne-Labarthet et al., 2004; Labarthet et al., 2004, 2000). The strong surface orientation is confirmed by photoelectron spectroscopy (Henneberg et al., 2004). What is found is that the chromophores orient perpendicular to the local polarization vector of the impinging interference pattern. Thus, for a $(+45^\circ, -45^\circ)$ two-beam interference: in the valleys $(x=0)$ the electric field is aligned in the y-direction, so the chromophores orient in the x-direction; in the peaks $(x=\Lambda/2)$ the chromophores orient in the y-direction; in the slope regions $(x=\Lambda/4)$ the electric field is circularly polarized and thus the chromophores are nearly isotropic. For a (p, p) two-beam interference, it is observed that the chromophores are primarily oriented in the y-direction everywhere, since the impinging light pattern is always linearly polarized in the x-direction. Mass transport may lead to perturbations in the orientational distribution, but photoorientation remains the dominant effect.

The anisotropy grating that is submerged below a SRG apparently leads to the formation of a density grating (DG) under appropriate conditions. It was found that upon annealing an SRG, which erases the surface grating and restores a flat film surface, a DG began growing beneath the surface (and into the film bulk) (Geue et al., 2002a; Pietsch et al., 2000). This DG only develops where the SRG was originally inscribed. It appears that the photoorientation and mass transport leads to the nucleation of LC "seeding aggregates" that are thermally grown into larger-scale density variations. The thermal erasure of the SRG, with concomitant growth of the DG, has been measured (Geue et al., 2003) and modeled (Pietsch, 2002). Separating the components because of the surface relief and the DG is described in a later section. Briefly, the diffraction of a visible light laser primarily probes the surface relief, whereas a simultaneous X-ray diffraction experiment probes the DG. The formation of a DG is similar to, and consistent with, the production of surface topography (Watanabe et al., 2000) and surface density patterns (Ikawa et al., 2000), as observed by tapping mode AFM, on an azo film exposed to an optical near field. In these experiments, it was found that volume is not strictly conserved during surface deformation (Keum et al., 2003), consistent with changes in density.

4.1.3. Dependence on Material Properties

For all-optical surface patterning to occur, one necessarily requires azobenzene chromophores in some form. There are, however, a wide variety of azo materials that have exhibited surface mass patterning. This makes the process much more attractive from an applied standpoint: it is not merely a curiosity restricted to a single system, but rather a fundamental phenomenon that can be engineered into a wide variety of materials. It was recognized early on that the gratings do not form in systems of small molecules (for instance, comparing unreacted monomers to their corresponding polymers). The polymer molecular weight (MW), however, must not be too large (Barrett et al., 1996). Presumably a large MW eventually introduces entanglements that act as cross-links, hindering polymer motion. Thus intermediate MW polymers ($\mathrm{MW} \sim 10^3$, arguably oligomers) are optimal. That having been said, there are many noteworthy counterexamples. Weak SRGs can be formed in polyelectrolyte multilayers, which are essentially cross-linked-polymer systems (He et al., 2000a,b; Lee et al., 2000; Wang et al., 1998). Efficient grating formation has also been demonstrated using an azo-cellulose with ultrahigh MW ($\mathrm{MW} \sim 10^7$) (Yang et al., 2002, 2001). In a high MW polypeptide ($\mathrm{MW} \sim 10^5$), gratings could be formed where the grating amplitude was dependent on the polymer conformation (Yang et al., 2003). Restricted conformations (α-helices and β-sheets) hindered SRG formation.

The opposite extreme has also been investigated: molecular glasses (amorphous nonpolymeric azos with bulky pendants) exhibited significant SRG formation (Chun et al., 2003; Kim et al., 2003; Nakano et al., 2002). In fact, the molecular version formed gratings more quickly than its corresponding polymer (Ando et al., 2003). Another set of experiments compared the formation of gratings in two related arrangements: (1) a thin film of polymer and small-molecule azo mixed together and (2) a layered system, where a layer of the small-molecule azo was deposited on top of the pure polymer (Ciuchi et al., 2002). The SRG was negligible in the layered case. Although the authors suggest that "layering" inhibits SRG formation, it may be interpreted that coupling to a host polymer matrix enhances mass transport, perhaps by providing rigidity necessary for fixation of the pattern. A copolymer study did in fact indicate that strong coupling of the mesogen to the polymer enhanced SRG formation (Naydenova et al., 1998b), and molecular glasses with hindered structures also enhanced grating formation (Ishow et al., 2006).

Gratings have also been formed in LC systems (Helgert et al., 2001; Holme et al., 1999). In some systems, it was found that adding stoichiometric quantities of a nonazo LC guest greatly improved the grating inscription (Ubukata et al., 2002, 2000). This suggests that SRG formation may be an inherently cooperative process, related to the mesogenic nature of the azo chromophore. The inscription sometimes requires higher power ($>1\,\mathrm{W/cm^2}$) than in amorphous systems (Ramanujam et al., 1996). In dendrimer systems, the quality of the SRG depends on the generation number (Archut et al., 1998).

Maximizing the content of azo chromophore usually enhances SRG formation (Fukuda et al., 2000a), although some studies have found that intermediate functionalization (50%–80%) created the largest SRG (Borger et al., 2005; Andruzzi et al., 1999). Some attempts have been made to probe the effect of free volume. By attaching substituents to the azo-ring, its steric bulk is increased, which presumably increases the free volume requirement for isomerization. However, substitution also invariably affects the isomerization rate constants, quantum yield, refractive index, etc. This makes any analysis ambiguous. At least in the case of photoorientation, the rate of inscription appears slower for bulkier chromophores, although the net orientation is similar (Ho et al., 1995; Natansohn et al., 1992). For grating formation, it would appear that chromophore bulk is of secondary importance to many other inscription parameters. The mass transport occurs readily at room temperature, which is well below the T_g of the amorphous polymers typically used. Gratings can even be formed in polymers with exceptionally high T_g (Lee et al., 1998), sometimes higher than 370°C (Chen et al., 1999). These gratings can sometimes be difficult to erase via annealing (Wu et al., 2001).

4.1.4. Photosoftening

The formation of an SRG involves massive material motion. It has been suggested that the process is in some way a surface phenomenon since nonazo capping layers tend to inhibit the phenomenon (Viswanathan et al., 1998). Many other experiments, however, confirm that azos deeper in the film (which still absorb light) contribute to the mass transport (Yager and Barrett, 2007; Geue et al., 2002c). It is clear that the azobenzene isomerization is necessary to permit bulk material flow well below the polymer T_g. It is often postulated that repeated trans → cis → trans cycles "photosoften" or "photoplasticize" the polymer matrix, enhancing polymer mobility by orders of magnitude. While compelling, this explanation has been difficult to directly observe. Clearly motion is enabled during isomerization, as demonstrated by mass transport, increases in gas permeability (Kameda et al., 2003), the segregation of some material components to the free surface (Sharma et al., 2002), and the ability to optically erase SRGs (Lagugne-Labarthet et al., 2002; Sanchez et al., 2000; Jiang et al., 1998). The fact that incoherent illumination during SRG inscription enhances grating formation may also be interpreted as evidence that photosoftening is a dominant requirement for mass transport (Yang et al., 2004). Numerous reports have confirmed a reduction in the viscosity of polymer solutions on trans to cis conversion (Moniruzzaman et al., 2004; Bhatnagar et al., 1995; Kumar et al., 1984). This photothinning can be attributed to both chain conformation (reduced hydrodynamic size) and interchain interactions. The extent to which such results can be extended into bulk films is debatable. It is also worth noting that a depression of T_g near the surface of a polymer film is now well established. (Forrest and Dalnoki-Veress, 2001). One might be tempted to explain the mass transport by suggesting that an ultrathin layer of polymer material at the surface is sufficiently mobile (below T_g) to move, thereby exposing "fresh surface," which then becomes mobile. However, the T_g depressions typically measured are not sufficient to account for the process (especially in high T_g samples). Moreover, this does not explain why the mass patterning is only observed in samples that contain azobenzene.

Despite compelling indirect experiments, there are few results that directly suggest photosoftening in bulk samples. Initial hints from AFM response (Kumar et al., 1998), experiments with a quartz crystal microbalance (Srikhirin et al., 2000), and electromechanical spectroscopy (Mechau et al., 2005, 2002; Srikhirin et al., 2000) all indicated that photosoftening occurred. However, the magnitude of the effect was found to be quite small ($<10\%$ change in modulus). Recent AFM modulus (Yager and Barrett, 2006b; Stiller et al., 2004) and tracer diffusion (Mechau et al., 2006) experiments have established that the softening is very small and certainly much smaller than the change in mechanical response that occurs upon heating a polymer to T_g. Thus, although mobility appears to be comparable to a polymer above T_g, other mechanical properties are only slightly modified. It may indeed be that isomerization merely enables localized molecular motion, but that the continual creation of molecular free volume pockets, which are then reoccupied by neighboring isomerizing chromophores, enables a net cooperative movement of material, akin to the displacement of a vacancy defect in a crystal or hole in a semiconductor (Mechau et al., 2002).

4.1.5. Photomechanical Effects

In light of the confounding photosoftening results, an area of increasing research is the direct study of photomechanical effects and macroscopic motion in azobenzene systems. A direct demonstration of macroscopic motion is the bending and unbending of freestanding LC azopolymer films (Ikeda et al., 2003; Yu et al., 2003). This effect is caused by a photocontraction of the free surface, with a decreasing contraction gradient into the depth of the material (as light intensity decreases because of absorption). Polarization can be used to control the direction of bending (Yu et al., 2005), suggesting possible optimization for photoactuation (Tabiryan et al., 2005). Recent measurements using both ellipsometry (Tanchak and Barrett, 2005) and neutron reflectivity (Yager et al., 2006a,b) have identified photoexpansion, on the order of 4%, in amorphous azopolymer films during irradiation. The expansion has both a reversible and irreversible component, suggesting both elastic deformation and viscoelastic flow play a role in azo mass transport. Contraction is observed in LC materials, whereas expansion observed in amorphous polymers is consistent with other investigations. For instance, for thin films floating on a water surface, a contraction in the direction of polarized light was seen in liquid crystal materials, whereas an expansion was observed for amorphous samples (Bublitz et al., 2000). Experiment combining neutron reflectometry and AFM identified both photoexpansion and photocontraction in a single material (Yager and Barrett, 2006b; Yager et al., 2006b). In particular, photoexpansion was observed at low temperatures, whereas photocontraction was observed at higher temperature, with a distinct crossover temperature (at $\sim 50°C$ for pdr1a). This suggests that material motion involves two competing mechanisms: one that causes material expansion (e.g., the internal pressure from the free volume required for azo isomerization) and one that causes material contraction (e.g., dipole pairing and crystallization of azo groups). At low temperatures (in amorphous materials), the rigidity of the matrix prevents the relaxation required for crystallization, and thus photoexpansion is frozen in place. However above a crossover temperature, mobility is sufficient for azo groups to reorganize and crystallize into higher density states. It may thus be that liquid crystal materials exhibit photocontraction simply because they are above their characteristic crossover temperature under normal measurement conditions. These results imply that mass transport can be explained within the framework of photomechanical effects.

4.1.6. Measuring Gratings

The formation of an SRG is typically monitored via the diffraction of a probe laser beam. One must be careful in analyzing this diffraction efficiency, however, because a number of simultaneous gratings will be generated in an azo sample during illumination with a light pattern (Fig. 4.6a–d). A light intensity pattern will lead to a chemical grating, since illuminated regions will be more cis rich than dark regions. The resultant spatial variation of absorbance and refractive index will lead to various optical effects, including diffraction. This grating is temporary,

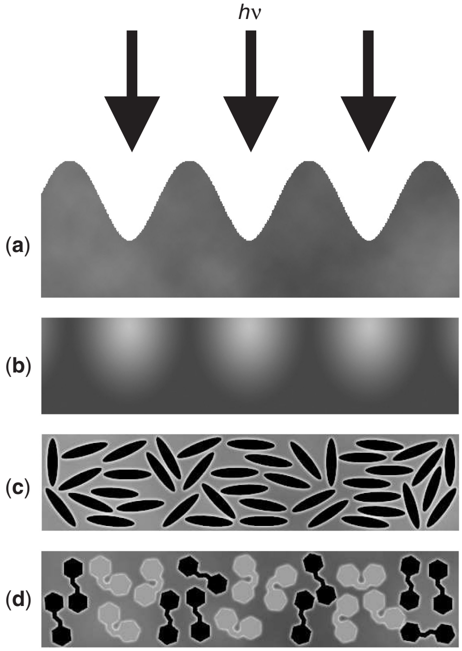

Figure 4.6. Schematic of the different gratings that are formed during illumination of an azo sample. (**a**) SRG. (**b**) DG. (**c**) Birefringence (orientational) grating. (**d**) Chemical (trans/cis) grating. All the gratings contribute to the observed diffraction efficiency, to varying extents. Gratings (**b**), (**c**) and (**d**) are all refractive-index gratings.

persisting only during irradiation. Simultaneously, a birefringence grating will be inscribed. These birefringence patterns are stable and contribute to the observed final diffraction efficiency. An SRG is of course induced if there is any spatial variation in intensity or polarization, and diffraction from this grating is very large, sometimes overwhelming other effects. Lastly, a DG appears to be seeded beneath the material surface, which will also lead to periodic variation of refractive index.

The contributions to diffraction due to the surface relief and birefringence gratings can be deconvoluted using a Jones matrix formalism applied to polarized measurements of the first-order diffracted beams (Helgert et al., 2000; Labarthet et al., 1999, 1998; Naydenova et al., 1998b; Holme et al., 1997). Similarly, scattering theory (Geue et al., 2002b; Pietsch, 2002) was used to fit visible light and X-ray diffraction data (Henneberg et al., 2003; Geue et al., 2002c, 2000; Henneberg et al., 2001b) to deconvolute contributions owing to surface relief and density (refractive index) gratings. For scattering from an SRG, the x and z components of the momentum transfer are

$$\begin{aligned} q_x &= k\left(\sin\theta_f - \sin\theta_i\right) \\ q_z &= nk\left(\cos\theta_i - \cos\theta_f\right) \end{aligned} \tag{4.2}$$

where θ_i and θ_f are the incident and reflected angles, and $k=2\pi/\lambda$. For the visible diffracted peak of order m (i.e., when $q_x=m2\pi/\Lambda$), the scattering intensity was derived to be

$$I_{\text{vis}} \approx \left|J_m(q_z h) - e^{iq_z d} J_m(q_z \Delta n_m d)\right|^2 \tag{4.3}$$

where d is the film thickness, h is the grating height, Δn_m is the mth Fourier component of the refractive-index grating, and J_m the mth Bessel function. These Bessel functions can give rise to oscillations in the diffraction signal (Fig. 4.7). Thus, one must be careful not to implicitly assume a linear dependence between grating amplitude and diffraction efficiency. Clearly, both the DG and SRG contribute to the signal. For the X-ray signal, the scattering amplitude is given by the following:

$$A_{\text{x-ray}} \approx J_m(q_z h) - e^{iq_z d}\frac{B_m}{2} \tag{4.4}$$

where one must now use the q_z appropriate for X-rays, and B_m represents the Fourier component of the density modulation (which is presumably identical to the index-modulation). The intensity is not simply the square of A, but can be determined using Fresnel transmission functions. The visible scattering is mostly sensitive to the surface-relief, and the X-ray scattering is due primarily to the density modulation. Using both measurements, the two contributions can of course be determined.

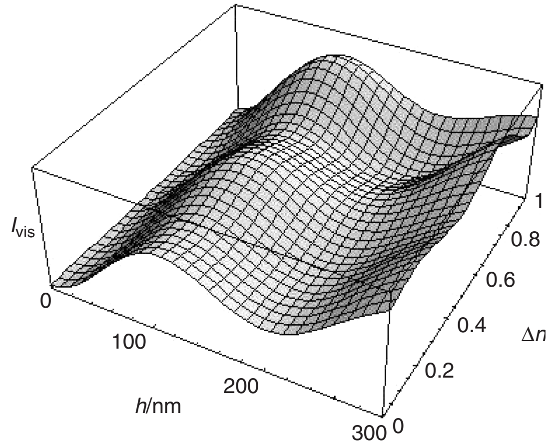

Figure 4.7. Diffraction intensity of a 700 nm thick film as a function of the inscribed grating height, *h*, and induced refractive-index grating (Δn) based on Equation 4.3. The diffraction intensity is not a linear function of either variable. Oscillations in the signal can complicate analysis of experiments.

It is noteworthy that chromophores may actually be disturbed by probe beams that are well outside of the azo absorption window. For instance, it was found that illumination using red light (outside of the azo absorption band) made DGs (formed underneath SRGs) stable against thermal erasure (Geue et al., 2002a). Others have found that chromophores become slowly aligned even with red laser light, where absorption should be nominal. Luckily the diffraction from azo gratings is intense, enabling the use of heavily attenuated probe beams.

4.1.7. Dynamics

The dynamics of SRG inscription have been the subject of many studies. To a first approximation, the inscription process does not depend on the temporal distribution of laser power, only on the net exposure. Yet this general rule breaks down at high and low power, and for short or interrupted exposures, revealing more complications inherent to the process. The inscription appears to be nonlinear, saturating with inscription time and power, and being dependent on history (Saphiannikova et al., 2004b). Interestingly, the growth of the gratings appears to continue for a short time after illumination has ceased, hinting at a photoinduced stress that persists in the dark. This may be due to the relatively slow decay of the cis population. For short (<2 s) moderate-power laser pulses, no permanent grating can be formed, even after repeated pulse exposure (Henneberg et al., 2001a). For longer (>5 s) pulses, material deformation can be seen after every exposure, and repeated exposure eventually leads to an SRG. These short pulses give rise to localized hills that eventually become a smooth sine wave. This implies that with sufficient power, individual azo chromophores or nanodomains deform, which when summed lead to a grating. Although short exposures do not form permanent gratings, some response is seen, possibly indicating elastic deformation (Geue et al., 2002c; Henneberg et al., 2001b) in addition to plastic flow.

The formation and erasure of surface relief and DGs in azo films has been measured and modeled. Using the formalism described in Section 4.1.6, one can fit the measured scattering by allowing h and Δn (or B_m) to vary in time. For instance, the erasure of the SRG, and concomitant enhancement and then disappearance of the X-ray signal, can be fit using (Geue et al., 2003) the following:

$$\begin{aligned} h &= h_{\max}\frac{1}{1+\exp\big((T-C_{\mathrm{SRG}}T_g)/E_{a,\mathrm{SRG}}\big)} \\ B &= B_{m,\max}\frac{1}{1+\exp\big((T-C_{\mathrm{DG}}T_g)/E_{a,\mathrm{DG}}\big)} \end{aligned} \tag{4.5}$$

where $E_{a,i}$ and C_i are the activation energy and a fitting parameter, respectively, for the SRG and DG. It is found that the SRG begins disappearing ~15 K before T_g. In contrast to this thermal erasure of SRGs, it appears that in some LC systems, thermal treatment after SRG formation leads to an enhancement of the grating height (Kawatsuki et al., 2003; Stracke et al., 2000). In these cases, heating may enable motion and aggregation of chromophores. Thin film confinement effects have also been observed. In particular, thin films cause an increase in the erasing temperature, equivalent to an increase of the apparent T_g by as much as 50 K (Yager and Barrett, 2007). The molecular-scale dynamics (e.g., isomerization) are negligibly affected by confinement, whereas the large-scale mass transport becomes arrested within ~150 nm of the substrate interface.

4.2. MECHANISM

Several mechanisms have been described to account for the microscopic origin of the driving force in azobenzene optical patterning. Arguments have appealed to thermal gradients, diffusion considerations, isomerization-induced pressure gradients, and interactions between azo dipoles and the electric field of the incident light. Considering the large body of experimental observations, it is perhaps surprising that the issue of mechanism has not yet been settled. At present, no mechanism appears to provide an entirely complete and satisfactory explanation consistent with all known observations. However, viscoelastic modeling of the process has been quite successful, correctly reproducing nearly all experimentally observed surface patterns, without directly describing the microscopic nature of the driving force. Fluid mechanics models provided suitable agreement with observations (Barrett et al., 1998) and were later extended to take into account a depth dependence and a velocity distribution in the film (Fukuda et al., 2000b; Sumaru et al., 1999), which reproduces the thickness dependence of SRG inscription. A further elaboration took into account induced anisotropy in the film and associated anisotropic polymer film deformation (expansion or contraction in the electric field direction) (Bublitz et al., 2001). The assumption of an anisotropic deformation is very much consistent with experimental observations (Bublitz et al., 2000). Such an analysis, remarkably, was able to reproduce most of the polarization dependence, predict phase-inverted behavior at high power, and even demonstrated double-period (interdigitated) gratings. A nonlinear stress-relaxation analysis could account for the nonlinear response during intermittent (pulselike) exposure (Saphiannikova et al., 2004b). Finite-element linear viscoelastic modeling enabled the inclusion of finite compressibility (Saphiannikova et al., 2004a). This allowed the nonlinear intermittent-exposure results, and, critically, the formation of DGs, to be correctly predicted. This analysis also demonstrated, as expected, that surface tension acts as a restoring force that limits grating amplitude (which explains the eventual saturation). Finally, the kinetics of grating formation (and erasure) have been captured in a lattice Monte Carlo simulation that takes into account isomerization kinetics and angular redistribution of chromophores (Mitus et al., 2004; Pawlik et al., 2004, 2003). Thus, the nonlinear viscoelastic flow and deformation (compression and expansion) of polymer material appear to be well understood. What remains to be fully elucidated is the origin of the force inside the material. More specifically, the connection between the azobenzene isomerization and the apparent force must be explained.

4.2.1. Thermal Considerations

Models involving thermal effects were proposed when SRG formation was first observed. Although simple and appealing, a purely thermal mechanism would not account for the polarization dependence that is observed experimentally. The grating formation proceeds at remarkably low laser power, thus thermal mechanisms appear untenable. A more detailed modeling analysis (Yager and Barrett, 2004) showed that the temperature gradient induced in a sample under typical SRG formation conditions was on the order of 10^{-4} K. This thermal gradient is much too small for any appreciable spatial variation of material properties. The net temperature rise in the sample was found to be on the order of 5 K, which again suggests that thermal effects (such as temperature-induced material softening) are negligible. However, high intensity experiments have shown the formation of gratings that could not be subsequently thermally erased (Bian et al., 1999). It is likely that in these cases a destructive thermal mechanism plays a role. In nanosecond-pulsed experiments, gratings can be formed (Si et al., 2002; Leopold et al., 2000; Ramanujam et al., 1999; Schmitt et al., 1997). However, these gratings are because of irreversible ablation of the sample surface, a phenomenon well established in high power laser physics. Moreover, the formation of gratings at these energies does not require azobenzene: any absorbing chromophore will do (Baldus et al., 2001). Computer modeling confirms temperature rises on the order of $\sim$8000 K for nanosecond pulses (Yager and Barrett, 2004), clearly an entirely different regime from the facile room temperature patterning unique to azo chromophores. Although thermal effects should be considered for a complete understanding of SRG formation (especially the phase-inverted structures observed at higher power), they appear to be negligible for typical irradiation conditions at modest laser power.

4.2.2. Asymmetric Diffusion

An elegant anisotropic translation mechanism was developed by Lefin, Fiorini, and Nunzi (Lefin et al., 1998a,b). In this model, material transport occurs essentially because of an (orientational) concentration gradient. It is suggested that the rapid cycling of chromophores between trans and cis states enables transient, random motion of molecules preferentially along their long axis, because of the inherent anisotropy of azo molecules. The probability of undergoing a random-walk step is proportional to the probability of isomerization, which of course depends on the light intensity and the angle between the chromophore dipole and the incident electric vector. This predicts a net flux of molecules out of the illuminated areas and into the dark regions, consistent with experiment. This process would be enhanced by pointing dipoles in the direction of the light gradient (toward the dark regions). This would appear to explain the polarization dependence to a certain extent. In contrast to experiment, however, this model implies the best results when using small molecules, not polymers. For polymer chains laden with many chromophores, random motion of these moeities would presumably lead to a "tug-of-war" that would defeat net transport of the chain. It is at present not clear that the driving force in this model is sufficient to account for the substantial mass transport (well below T_g) observed in experiments.

4.2.3. Mean-Field Theory

Mechanisms based on electromagnetic forces are promising since they naturally include the intensity and polarization state of the incident light field. In the mean-field model developed by Pedersen and coworkers (Pedersen et al., 1998; Pedersen and Johansen, 1997), each chromophore is subject to a potential resulting from all the other chromophore dipoles in the material. Irradiation orients chromophores, and this net orientation leads to a potential that naturally aligns other chromophores. Furthermore, there is an attractive force between side-by-side chromophores that are aligned similarly. This leads to a net force on chromophores in illuminated areas, causing them to order and aggregate. Obviously this model predicts an accumulation of chromophores in the illuminated areas. Thus surface relief peaks will be aligned with light intensity maxima. Although this result does not agree with experiments in amorphous samples, it is consistent with many experiments on LC systems. The mean-field model inherently includes intermolecular cooperativity and orientational order, and it appears natural that it would be manifest in mobile LC systems. The polarization state of incident light is explicitly included in the model, as it serves to align dipoles and thus enhance the mean-field force. Because of this, even pure polarization patterns lead to gratings in this model. This mechanism appeals to the unique properties of azobenzenes only to explain the photoorientation of dipoles. If this mechanism were general, one would expect it to operate on nonisomerizing dipoles that had been aligned by other means, which has not yet been observed.

4.2.4. Permittivity Gradient Theory

A mechanism involving spatial variation of the permittivity, ε, has been suggested by Baldus and Zilker (2001). This model assumes that a spatial modulation of the refractive index, hence permittivity, is induced in the film. This is certainly reasonable, given the well-known photoorientation and birefringence gratings in azo systems. A force is then exerted between the optical electric field and the gradient in permittivity. Specifically, the force is proportional to the intensity of the electric field in the mass transport direction and to the gradient of the permittivity:

$$\vec{f} = -\frac{\varepsilon_0}{2}\vec{E}^2\nabla\varepsilon \tag{4.6}$$

Mass is thus driven out of areas with a strong gradient in ε, which generally moves material into the dark (consistent with the phase relationship in amorphous systems). Here again the mechanism appears general: any system with spatial variation of refractive index should be photopatternable, yet this is not observed. This model would appear to require that adequate photoorientation precede mass transport. Most experiments indicate, however, that both orientational and surface relief phenomena begin immediately and continue concurrently throughout inscription. This model was used to explain SRG formation in pulsed experiments (Baldus et al., 2001; Leopold et al., 2000), where thermal effects were suggested as giving rise to the spatial variation of permittivity, but the resulting force was essentially identical. However, conventional laser ablation appears to be a simpler explanation for those results (Yager and Barrett, 2004).

4.2.5. Gradient Electric Force

Kumar and coworkers proposed a mechanism on the basis of the observation that an electric field component in the direction of mass flow was required (Yang et al., 2006; Bian et al., 2000; Viswanathan et al., 1999a; Kumar et al., 1998). This force is essentially an optical gradient force (Chaumet and Nieto-Vesperinas, 2000; Ashkin, 1997, 1970). Spatial variation of light (electric field intensity and orientation) leads to a variation of the material susceptibility, χ, at the sample surface. The electric field then polarizes the material. The induced polarization is related to the light intensity and local susceptibility:

$$\vec{P}_i = \varepsilon_0\chi_{ij}\vec{E}_j \tag{4.7}$$

Forces then occur between the polarized material and the light field, analogous to the net force on an electric dipole in an electric field gradient. The time-averaged force was derived to be (Viswanathan et al., 1999a) as follows:

$$\vec{f} = \left\langle (\vec{P} \cdot \nabla)\vec{E} \right\rangle \tag{4.8}$$

The grating inscription is related to the spatially varying material susceptibility, the magnitude of the electric field, and the gradient of the electric field. This theory was extended to include near-field optical gradient forces, which have been used for patterning in some experiments (Ikawa et al., 2001). The gradient force model naturally includes the polarization dependence of the incident light, and reproduces essentially all of the polarization features of single-beam and SRG experiments. It has been pointed out (Natansohn and Rochon, 2002), however, that another analysis (Gordon, 1973) of forces exerted on polarizable media suggested a dependence on the gradient of the electric field, but not its polarization direction. The gradient force theory requires azobenzene photochemistry to modulate susceptibility via photoorientation and also implicitly assumes that photoplasticization is enabling mass transport. It would appear, however, that the force density predicted by this model is much too small to account for mass transport in real systems. A straightforward analysis presented by Saphiannikova et al. (2004a) is described here. In the case of two circularly polarized beams (for instance), the force acting in the x-direction, according to the gradient electric force model, would be

$$f = -k\varepsilon_0 \chi E_0^2 \sin\theta (1 + \cos^2\theta) \sin(kx \sin\theta) \tag{4.9}$$

where 2θ is the angle between the two beams and $k = 2\pi/\lambda$. Since ${E_0}^2 = 2Iz_0$, where z_0 is the vacuum impedance and I is the light intensity, the maximum expected force is

$$f_{\max} = \frac{4\pi}{\lambda} \varepsilon_0 z_0 \chi I \tag{4.10}$$

Given that $\varepsilon_0 = 8.854 \times 10^{-12} \mathrm{C}^2/(\mathrm{Nm}^2)$, $|\chi| \approx 1$ and $z_0 = 377\,\Omega$, and using the typical values $I = 100\,\mathrm{mW/cm}^2$ and $\lambda = 488\,\mathrm{nm}$, a force density of $\sim 100\,\mathrm{N/m}^3$ is obtained. Not only are these two orders of magnitude smaller than the force of gravity (which itself is presumably negligible), but they also fall short of the estimated 10^{11}–$10^{14}\,\mathrm{N/m}^3$ necessary for mass transport in polymer films to occur (Saphiannikova et al., 2004a).

4.2.6. Isomerization Pressure

One of the first mechanisms to be presented was the suggestion by Barrett et al. (1998, 1996) about pressure gradients inside the polymer film. The assumption is that azobenzene isomerization generates pressure both because of the greater free volume requirement of the cis and the volume requirement of the isomerization process itself. Isomerization of the bulky chromophores leads to pressure that is proportional to light intensity. The light intensity gradient thus generates a pressure gradient, which of course leads to material flow in a fluid mechanics treatment. Order-of-magnitude estimates were used to suggest that the mechanical force of isomerization would be greater than the yield point of the polymer, enabling flow. Plastic flow is predicted to drive material out of the light, consistent with observations in amorphous systems. At first it would seem that this mechanism cannot be reconciled with the polarization dependence, since the pressure is presumably proportional to light intensity, irrespective of its polarization state. However, one must more fully take orientational effects into account. Linearly polarized light addresses fewer chromophores than circularly polarized light and would thus lead to lower pressure. Thus, pure polarization patterns can still lead to pressure gradients. Combined with the fact that the polarized light is orienting (and in a certain sense photobleaching), this can explain some aspects of the polarization data. The agreement, however, is not perfect. For instance, the (*s*, *s*) and (*p*, *p*) combinations lead to very different gratings in experiments. It is possible that some missing detail related to polarization will help explain this discrepancy.

Combining a variety of results from the literature, it now appears that the mechanical argument of a pressure mechanism may be correct. In one experiment, irradiation of a transferred Langmuir–Blodgett film reversibly generated ~5 nm "hills," attributed to nanoscale buckling that relieves the stress induced by lateral expansion (Matsumoto et al., 1998). This result is conspicuously similar to the spontaneous polarization-dependent formation of hexagonally arranged ~500 nm hills seen on an amorphous azopolymer sample irradiated homogeneously (Hubert et al., 2002a,b). In fact, homogeneous illumination of azo surfaces has caused roughening (Mechau et al., 2002), and homogeneous optical erasure of SRGs leads to similar pattern formation (Lagugne-Labarthet et al., 2002). The early stages of SRG formation, imaged by AFM, again show the formation of nanosized hills (Henneberg et al., 2001a). Taken together, these seem to suggest that irradiation of an azo film leads to spontaneous lateral expansion, which induces a stress that can be relieved by buckling of the surface, thereby generating surface structures. In the case of a light gradient, the buckling is relieved by mass transport coincident with the light field that generated the pressure inside the film. In an experiment on main-chain versus side-chain azopolymers, the polarization behavior of photodeformation was opposite (Keum et al., 2003). This may be explained by postulating that the main-chain polymer contracts upon isomerization, whereas the side-chain polymer architecture leads to net expansion. Similarly, the opposite phase behavior in amorphous and LC systems may be due to the fact that the former photoexpand and the latter photocontract (Bublitz et al., 2000). Lastly, many large surface structures were observed in an azo-dye-doped elastomer film irradiated at high power ($4\,\mathrm{W/cm^2}$) (Ciuchi et al., 2003). The formation of structures both parallel and perpendicular to the grating direction could be attributed to photoaggregation of the azo dye molecules or buckling of the elastomeric surface. Indeed all of these otherwise contradictory results can be reconciled by considering a more general photomechanical explanation, where both photoexpansion (for materials below a crossover mobility temperature; i.e., amorphous) and photocontraction (for materials above a mobility threshold; i.e., liquid crystal samples) both occur (Yager and Barrett, 2006b). Further investigations into reconciling this model with the polarization dependence of inscription are in order, where presumably photoorientation will play a key role.

4.2.7. Applications of Surface Mass Transport

The single-step, rapid, and reversible all-optical surface patterning effect discovered in a wide variety of azobenzene systems has, of course, been suggested as the basis for numerous applications. Azobenzene is versatile, amenable to incorporation in a wide variety of materials. The mass patterning is reversible, which is often advantageous. However, one may use a system where cross-linking enables permanent fixation of the surface patterns (Zettsu et al., 2001). Many proposed applications are optical and fit well with azobenzene's already extensive list of optical capabilities. The gratings have been demonstrated as optical polarizers (Tripathy et al., 2000), angular or wavelength filters (Stockermans and Rochon, 1999; Rochon et al., 1997), and couplers for optical devices (Paterson et al., 1996). They have also been suggested as photonic band gap materials (Nagata et al., 2001), and have been used to create lasers where emission wavelength is tunable via grating pitch (Rocha et al., 2001; Dumarcher et al., 2000). The process has, of course, been suggested as an optical data storage mechanism (Egami et al., 2000). The high speed and single-step holographic recording has been suggested to enable "instant holography" (Ramanujam et al., 1999), with obvious applications for industry or end consumers. Since the hologram is topographical, it can easily be used as a master to create replicas via molding. The surface patterning also allows multiple holograms to be superimposed, if desired. A novel suggestion is to use the patterning for rapid prototyping of optical elements (Neumann et al., 1999). Optical elements could be generated or modified quickly and during device operation. They could thereafter be replaced with permanent components, if required.

The physical structure of the surface relief can be exploited to organize other systems. For instance, it can act as a command layer, aligning liquid crystals (Kaneko et al., 2002; Parfenov et al., 2001, 2000; Kim et al., 2000; Li et al., 1999). The grating can be formed after the LC cell has been assembled and can be erased and rewritten. Colloids can also be arranged into the grooves of an SRG, thereby templating higher order structures (Yi et al., 2002a, 2001). These lines of colloids can then be sintered to form wires (Yi et al., 2002b). The surface topography inscription process is clearly amenable to a variety of optical-lithography patterning schemes. These possibilities will hopefully be more thoroughly investigated. An advantage of holographic patterning is that there is guaranteed registry between features over macroscopic distances. This is especially attractive as technologies move toward wiring nanometer-sized components. One example in this direction involved evaporating metal onto an SRG, and then annealing. This formed a large number of very long (several millimeter) but extremely thin (200 nm) parallel metal wires (Noel et al., 1996). Of interest for next-generation patterning techniques is the fact that the azo surface modification is amenable to near-field patterning, which enables high resolution nanopatterning by circumventing the usual diffraction limit of far-field optical systems. Proof of principle was demonstrated by irradiating through polystyrene spheres assembled on the surface of an azo film. This results in a polarization-dependent surface topography pattern (Watanabe et al., 2000) and a corresponding surface density pattern (Ikawa et al., 2000). Using this technique, resolution on the order of 20 nm was achieved (Hasegawa et al., 2001). This process appears to be enhanced by the presence of gold nanoislands (Hasegawa et al., 2002). It was also shown that volume is not strictly conserved in these surface deformations (Keum et al., 2003). In addition to being useful as a subdiffraction limit patterning technique, it should be noted that this is also a useful technique for imaging the near field of various optical interactions (Fukuda et al., 2001). The (as of yet not fully explained) fact that subdiffraction limit double-frequency SRGs can be inscribed via far-field illumination (Lagugne-Labarthet et al., 2004; Labarthet et al., 2001, 2000; Naydenova et al., 1998a) further suggests the azopolymers as versatile high resolution patterning materials.

4.3. CONCLUSIONS

The azobenzene chromophore is a unique molecular switch, exhibiting a clean and reversible photoisomerization that induces a reversible change in geometry (Yager and Barrett, 2006a). This motion can be exploited as a photoswitch, and amplified so that larger-scale material properties are switched or altered in response to light. Thus, azo materials offer a promising potential as photomechanical materials. In addition to being useful in a variety of photoswitching roles, the azobenzene isomerization, being fundamentally a geometrical motion, can give rise to many types of motion. These motions can lead to formation of structures at a variety of length scales, from molecular to macroscopic. Furthermore, the formation of these structures is optically controlled, which is very attractive to modern industry. At a molecular level, there is much promise in exploiting azobenzenes to control the organization of nanomaterials and the functioning of nanomechanical devices. At a nanometer level, these materials can be used to form arbitrary surface patterns in a single-step process. At a macroscopic level, the motion could be exploited in a variety of photoactuators and artificial muscles.

With regard to the mechanism of surface mass transport, there is a need for further theory and experiments. An emerging possibility is that two competing mechanisms apply at different power levels. In some systems, notably LC ones, motion is sufficiently free that the "high power" mechanism is readily accessible.

Such an interpretation seems to resolve the apparent conflict between many different results. The nature of the two mechanisms, of course, remains an open question. The high power mechanism may be because of mean-field forces. Again, in mobile LC systems, or at sufficient power, one might expect molecules to align, attract one another, and move cooperatively. In the low power regime, a photomechanical mechanism appears tenable, although polarization questions need to be addressed, presumably by appealing to photoorientation phenomena. From an applied perspective, the azopolymers are well suited for some types of high performance optical lithography. Specifically, these materials have been patterned at the subdiffraction limit level, thus showing that any material resolution limits are below the usual optical limits. The double period gratings that have been produced show that these systems are amenable to subdiffraction limit patterning even with far-field illumination. Ongoing research is evaluating these effects in terms of facile optical formation of nanostructures.

ACKNOWLEDGMENT

This work is dedicated to professors Almeria Natansohn and Sukant Tripathy, teachers and pioneers in the field of azopolymers, who were unable to see the completion of this book.

REFERENCES

Ando H, Takahashi T, Nakano H, Shirota Y. 2003. Comparative studies of the formation of surface relief grating amorphous molecular material vs vinyl polymer. Chem Lett 32(8):710–711.

Andruzzi L, et al. 1999. Holographic gratings in azobenzene side-chain polymethacrylates. Macromolecules 32(2):448–454.

Archut A, et al. 1998. Azobenzene-functionalized cascade molecules: photoswitchable supramolecular systems. Chem Eur J 4(4):699–706.

Ashkin A. 1970. Acceleration and trapping of particles by radiation pressure. Phys Rev Lett 24(4):156–159.

Ashkin A. 1997. Optical trapping and manipulation of neutral particles using lasers. Proc Natl Acad Sci USA 94(10):4853–4860.

Baldus O, Zilker SJ. 2001. Surface relief gratings in photoaddressable polymers generated by cw holography. Appl Phys B-Lasers O 72(4):425–427.

Baldus O, Leopold A, Hagen R, Bieringer T, Zilker SJ. 2001. Surface relief gratings generated by pulsed holography: a simple way to polymer nanostructures without isomerizing side-chains. J Chem Phys 114(3):1344–1349.

Barrett CJ, Natansohn AL, Rochon PL. 1996. Mechanism of optically inscribed high-efficiency diffraction gratings in Azo polymer films. J Phys Chem 100(21):8836–8842.

Barrett CJ, Rochon PL, Natansohn AL. 1998. Model of laser-driven mass transport in thin films of dye-functionalized polymers. J Chem Phys 109(4):1505–1516.

Bhatnagar A, et al. 1995. Azoaromatic polyethers. Polymer 36(15):3019–3025.

Bian S, et al. 1998. Single laser beam-induced surface deformation on azobenzene polymer films. Appl Phys Lett 73(13):1817–1819.

Bian SP, et al. 1999. Photoinduced surface deformations on azobenzene polymer films. J Appl Phys 86(8):4498–4508.

Bian SP, et al. 2000. Photoinduced surface relief grating on amorphous poly(4-phenylazophenol) films. Chem Mater 12(6):1585–1590.

Borger V, et al. 2005. Novel polymers to study the influence of the azobenzene content on the photo-induced surface relief grating formation. Macromol Chem Phys 206(15):1488–1496.

Bublitz D, et al. 2000. Photoinduced deformation of azobenzene polyester films. Appl Phys B: Lasers Opt 70(6):863–865.

Bublitz D, Fleck B, Wenke L. 2001. A model for surface-relief formation in azobenzene polymers. Appl Phys B-Lasers O 72(8):931–936.

Chaumet PC, Nieto-Vesperinas M. 2000. Time-averaged total force on a dipolar sphere in an electromagnetic field. Opt Lett 25(15):1065–1067.

Chen JP, Labarthet FL, Natansohn A, Rochon P. 1999. Highly stable optically induced birefringence and holographic surface gratings on a new azocarbazole-based polyimide. Macromolecules 32(25):8572–8579.

Chun CM, Kim MJ, Vak D, Kim DY. 2003. A novel azobenzene-based amorphous molecular material with a spiro linked bifluorene. J Materials Chem 13(12):2904–2909.

Ciuchi F, Mazzulla A, Cipparrone G. 2002. Permanent polarization gratings in elastomer azo-dye systems: comparison of layered and mixed samples. J Opt Soc Am B 19(11):2531–2537.

Ciuchi F, Mazzulla A, Carbone G, Cipparrone G. 2003. Complex structures of surface relief induced by holographic recording in azo-dye-doped elastomer thin films. Macromolecules 36(15):5689–5693.

Delaire JA, Nakatani K. 2000. Linear and nonlinear optical properties of photochromic molecules and materials. Chem Rev 100(5):1817–1846.

Dumarcher V, et al. 2000. Polymer thin-film distributed feedback tunable lasers. J Opt A: Pure Appl Opt 2(4):279–283.

Egami C, et al. 2000. Two-stage optical data storage in azo polymers. Jpn J Appl Phys 1 39(3B):1558–1561.

Forrest JA, Dalnoki-Veress K. 2001. The glass transition in thin polymer films. Adv Colloid Interface Sci 94(1–3):167–196.

Fukuda T, et al. 2000a. Photofabrication of surface relief grating on films of azobenzene polymer with different dye functionalization. Macromolecules 33(11):4220–4225.

Fukuda T, Sumaru K, Yamanaka T, Matsuda H. 2000b. Photo-induced formation of the surface relief grating on azobenzene polymers: analysis based on the fluid mechanics. Mol Cryst Liq Cryst 345:587–592.

Fukuda T, et al. 2001. Observation of optical near-field as photo-induced surface relief formation. Jpn J Appl Phys 2 40(8B):L900–L902.

Geue T, et al. 2000. X-ray investigations of the molecular mobility within polymer surface gratings. J Appl Phys 87(11):7712–7719.

Geue T, et al. 2002a. Formation of a buried density grating on thermal erasure of azobenzene polymer surface gratings. Coll Surf A 198–200:31–36.

Geue T, Henneberg O, Pietsch U. 2002b. X-ray reflectivity from sinusoidal surface relief gratings. Cryst Res Technol 37(7):770–776.

Geue TM, et al. 2002c. Formation mechanism and dynamics in polymer surface gratings. Phys Rev E 65(5):052801.

Geue TM, et al. 2003. X-ray investigations of formation efficiency of buried azobenzene polymer density gratings. J Appl Phys 93(6):3161–3166.

Gordon JP. 1973. Radiation Forces and Momenta in Dielectric Media. Phys Rev A 8(1):14–21.

Hasegawa M, Ikawa T, Tsuchimori M, Watanabe O, Kawata Y. 2001. Topographical nanostructure patterning on the surface of a thin film of polyurethane containing azobenzene moiety using the optical near field around polystyrene spheres. Macromolecules 34(21):7471–7476.

Hasegawa M, Keum C-D, Watanabe O. 2002. Enhanced photofabrication of a surface nanostructure on azobenzene-functionalized polymer films with evaporated gold Nanoislands. Adv Mater 14(23):1738–1741.

He J-A, et al. 2000a. Photochemical behavior and formation of surface relief grating on self-assembled polyion/dye composite film. J Phys Chem B 104(45):10513–10521.

He J-A, et al. 2000b. Surface relief gratings from electrostatically layered azo dye films. Appl Phys Lett 76(22):3233–3235.

Helgert M, Fleck B, Wenke L, Hvilsted S, Ramanujam PS. 2000. An improved method for separating the kinetics of anisotropic and topographic gratings in side-chain azobenzene polyesters. Appl Phys B-Lasers O 70(6):803–807.

Helgert M, Wenke L, Hvilsted S, Ramanujam PS. 2001. Surface relief measurements in side-chain azobenzene polyesters with different substituents. Appl Phys B: Lasers Opt 72(4):429–433.

Henneberg O, et al. 2001a. Atomic force microscopy inspection of the early state of formation of polymer surface relief gratings. Appl Phys Lett 79(15):2357–2359.

Henneberg O, et al. 2001b. Formation and dynamics of polymer surface relief gratings. Appl Surf Sci 182(3–4):272–279.

Henneberg O, Geue T, Rochon P, Pietsch U. 2003. X-ray and VIS light scattering from light-induced polymer gratings. J Phys D Appl Phys 36(10A):A241–A244.

Henneberg O, Geue T, Pietsch U, Saphiannikova M, Winter B. 2004. Investigation of azobenzene side group orientation in polymer surface relief gratings by means of photoelectron spectroscopy. Appl Phys Lett 84(9):1561–1563.

Ho MS, Natansohn A, Rochon P. 1995. Azo polymers for reversible optical storage 7. The effect of the size of the photochromic groups. Macromolecules 28(18):6124–6127.

Holme NCR, Nikolova L, Ramanujam PS, Hvilsted S. 1997. An analysis of the anisotropic and topographic gratings in a side-chain liquid crystalline azobenzene polyester. Appl Phys Lett 70(12):1518–1520.

Holme NCR, et al. 1999. Optically induced surface relief phenomena in azobenzene polymers. Appl Phys Lett 74(4):519–521.

Hore DK, Natansohn AL, Rochon PL. 2003. Anomalous cis isomer orientation in a liquid crystalline azo polymer on irradiation with linearly-polarized light. J Phys Chem B 107(10):2197–2204.

Hubert C, Fiorini-Debuisschert C, Maurin I, Nunzi JM, Raimond P. 2002a. Spontaneous patterning of hexagonal structures in an azo-polymer using light-controlled mass transport. Adv Mater 14(10):729.

Hubert C, et al. 2002b. Micro structuring of polymers using a light-controlled molecular migration processes. Appl Surf Sci 186(1–4):29–33.

Ikawa T, et al. 2000. Optical near field induced change in viscoelasticity on an azobenzene-containing polymer surface. J Phys Chem B 104(39):9055–9058.

Ikawa T, et al. 2001. Azobenzene polymer surface deformation due to the gradient force of the optical near field of monodispersed polystyrene spheres. Phys Rev B 64(19).

Ikeda T, Nakano M, Yu Y, Tsutsumi O, Kanazawa A. 2003. Anisotropic bending and unbending behavior of azobenzene liquid-crystalline gels by light exposure. Adv Mater 15(3):201–205.

Ishow E, et al. 2006. Structural and photoisomerization cross studies of polar photochromic monomeric glasses forming surface relief gratings. Chem Mater 18(5):1261–1267.

Jager C, Bieringer T, Zilker SJ. 2001. Bicolor surface reliefs in azobenzene side-chain polymers. Appl Opt 40(11):1776–1778.

Jiang XL, Kumar J, Kim DY, Shivshankar V, Tripathy SK. 1996. Polarization dependent recordings of surface relief gratings on azobenzene containing polymer films. Appl Phys Lett 68(19):2618–2620.

Jiang XL, Li L, Kumar J, Kim DY, Tripathy SK. 1998. Unusual polarization dependent optical erasure of surface relief gratings on azobenzene polymer films. Appl Phys Lett 72(20):2502–2504.

Kameda M, Sumaru K, Kanamori T, Shinbo T. 2003. Photoresponse gas permeability of azobenzene-functionalized glassy polymer films. J Appl Polym Sci 88(8):2068–2072.

Kaneko F, et al. 2002. Photo-induced fabrication of surface relief gratings in alternate self-assembled films containing azo dye and alignments of LC molecules. Coll Surf A 198:805–810.

Kawatsuki N, Uchida E, Ono H. 2003. Formation of pure polarization gratings in 4-methoxyazobenzene containing polymer films using off-resonant laser light. Appl Phys Lett 83(22):4544–4546.

Keum CD, Ikawa T, Tsuchimori M, Watanabe O. 2003. Photodeformation behavior of photodynamic polymers bearing azobenzene moieties in their main and/or side chain. Macromolecules 36(13):4916–4923.

Kim DY, et al. 1995a. Polarized laser induced holographic surface relief gratings on polymer films. Macromolecules 28(26):8835–8839.

Kim DY, Tripathy SK, Li L, Kumar J. 1995b. Laser-induced holographic surface relief gratings on nonlinear optical polymer films. Appl Phys Lett 66(10):1166–1168.

Kim DY, et al. 1997. Photo-fabrication of surface relief gratings on polymer films. Macromol Symp 116:127–134.

Kim M-H, Kim J-D, Fukuda T, Matsuda H. 2000. Alignment control of liquid crystals on surface relief gratings. Liq Cryst 27(12):1633–1640.

Kim M-J, Seo E-M, Vak D, Kim D-Y. 2003. Photodynamic properties of azobenzene molecular films with triphenylamines. Chem Mater 15(21):4021–4027.

Kumar GS, DePra P, Zhang K, Neckers DC. 1984. Chelating copolymers containing photosensitive functionalities. 2. Macromolecules 17(12):2463–2467.

Kumar J, et al. 1998. Gradient force: the mechanism for surface relief grating formation in azobenzene functionalized polymers. Appl Phys Lett 72(17):2096–2098.

Labarthet FL, Buffeteau T, Sourisseau C. 1998. Analyses of the diffraction efficiencies, birefringence, and surface relief gratings on azobenzene-containing polymer films. J Phys Chem B 102(15):2654–2662.

Labarthet FL, Rochon P, Natansohn A. 1999. Polarization analysis of diffracted orders from a birefringence grating recorded on azobenzene containing polymer. Appl Phys Lett 75(10):1377–1379.

Labarthet FL, et al. 2000. Photoinduced orientations of azobenzene chromophores in two distinct holographic diffraction gratings as studied by polarized Raman confocal microspectrometry. Phys Chem Chem Phys 2(22):5154–5167.

Labarthet FL, Buffeteau T, Sourisseau C. 2001. Time dependent analysis of the formation of a half-period surface relief grating on amorphous azopolymer films. J Appl Phys 90(7):3149–3158.

Labarthet FL, Bruneel JL, Buffeteau T, Sourisseau C. 2004. Chromophore orientations upon irradiation in gratings inscribed on azo-dye polymer films: a combined AFM and confocal Raman microscopic study. J Phys Chem B 108(22):6949–6960.

Lagugne-Labarthet F, Buffeteau T, Sourisseau C. 2002. Optical erasures and unusual surface reliefs of holographic gratings inscribed on thin films of an azobenzene functionalized polymer. Phys Chem Chem Phys 4(16):4020–4029.

Lagugne-Labarthet F, Bruneel JL, Rodriguez V, Sourisseau C. 2004. Chromophore orientations in surface relief gratings with second-order nonlinearity as studied by confocal polarized Raman microspectrometry. J Phys Chem B 108(4):1267–1278.

Lee S-H, et al. 2000. Azo polymer multilayer films by electrostatic self-assembly and layer-by-layer post azo functionalization. Macromolecules 33(17):6534–6540.

Lee TS, et al. 1998. Photoinduced surface relief gratings in high-Tg main-chain azoaromatic polymer films. J Polym Sci, Part A: Polym Chem 36(2):283–289.

Lefin P, Fiorini C, Nunzi JM. 1998a. Anisotropy of the photo-induced translation diffusion of azobenzene dyes in polymer matrices. Pure Appl Opt 7(1):71–82.

Lefin P, Fiorini C, Nunzi JM. 1998b. Anisotropy of the photoinduced translation diffusion of azo-dyes. Opt Mater 9(1–4):323–328.

Leopold A, et al. 2000. Thermally induced surface relief gratings in azobenzene polymers. J Chem Phys 113(2):833–837.

Li XT, Natansohn A, Rochon P. 1999. Photoinduced liquid crystal alignment based on a surface relief grating in an assembled cell. Appl Phys Lett 74(25):3791–3793.

Matsumoto M, et al. 1998. Reversible light-induced morphological change in Langmuir-Blodgett films. J Am Chem Soc 120(7):1479–1484.

Mechau N, Neher D, Borger V, Menzel H, Urayama K. 2002. Optically driven diffusion and mechanical softening in azobenzene polymer layers. Appl Phys Lett 81(25): 4715–4717.

Mechau N, Saphiannikova M, Neher D. 2005. Dielectric and mechanical properties of azobenzene polymer layers under visible and ultraviolet irradiation. Macromolecules 38(9):3894–3902.

Mechau N, Saphiannikova M, Neher D. 2006. Molecular tracer diffusion in thin azobenzene polymer layers. Appl Phys Lett 89(25):251902–3.

Mitus AC, Pawlik G, Miniewicz A, Kajzar F. 2004. Kinetics of diffraction gratings in a polymer matrix containing azobenzene chromophores: experiment and Monte Carlo simulations. Mol Cryst Liq Cryst 416:113–126.

Moniruzzaman M, Sabey CJ, Fernando GF. 2004. Synthesis of azobenzene-based polymers and the in-situ characterization of their photoviscosity effects. Macromolecules 37(7):2572–2577.

Nagata T, Matsui T, Ozaki M, Yoshino K, Kajzar F. 2001. Novel optical properties of conducting polymer-photochromic polymer systems. Synth Met 119(1–3):607–608.

Nakano H, Takahashi T, Kadota T, Shirota Y. 2002. Formation of a surface relief grating using a novel azobenzene-based photochromic amorphous molecular material. Adv Mater 14(16):1157–1160.

Natansohn A, Rochon P. 2002. Photoinduced motions in azo-containing polymers. Chem Rev 102(11):4139–4176.

Natansohn A, Xie S, Rochon P. 1992. Azo polymers for reversible optical storage 2. Poly[4′-[[2-(acryloyloxy)ethyl]ethylamino]-2-chloro-4-nitroazobenzene]. Macromolecules 25(20):5531–5532.

Naydenova I, et al. 1998a. Diffraction from polarization holographic gratings with surface relief in side-chain azobenzene polyesters. J Opt Soc Am B 15(4):1257–1265.

Naydenova I, et al. 1998b. Polarization holographic gratings with surface relief in amorphous azobenzene containing methacrylic copolymers. Pure Appl Opt 7(4):723–731.

Neumann J, Wieking KS, Kip D. 1999. Direct laser writing of surface reliefs in dry, self-developing photopolymer films. Appl Opt 38(25):5418–5421.

Noel S, Batalla E, Rochon P. 1996. A simple method for the manufacture of mesoscopic metal wires. J Mater Res 11(4):865–867.

Parfenov A, Tamaoki N, Ohnishi S. 2000. Photoinduced alignment of nematic liquid crystal on the polymer surface microrelief. J Appl Phys 87(4):2043–2045.

Parfenov A, Tamaoki N, Ohni-Shi S. 2001. Photoinduced alignment of nematic liquid crystal on the polymer surface microrelief. Mol Cryst Liq Cryst 359:487–495.

Paterson J, Natansohn A, Rochon P, Callendar CL, Robitaille L. 1996. Optically inscribed surface relief diffraction gratings on azobenzene-containing polymers for coupling light into slab waveguides. Appl Phys Lett 69(22):3318–3320.

Pawlik G, Mitus AC, Miniewicz A, Kajzar F. 2003. Kinetics of diffraction gratings formation in a polymer matrix containing azobenzene chromophores: experiments and Monte Carlo simulations. J Chem Phys 119(13):6789–6801.

Pawlik G, Mitus AC, Miniewicz A, Kajzar F. 2004. Monte Carlo simulations of temperature dependence of the kinetics of diffraction gratings formation in a polymer matrix containing azobenzene chromophores. J Nonlinear Opt Phy Mater 13(3–4): 481–489.

Pedersen TG, Johansen PM. 1997. Mean-field theory of photoinduced molecular reorientation in azobenzene liquid crystalline side-chain polymers. Phys Rev Lett 79(13): 2470–2473.

Pedersen TG, Johansen PM, Holme NCR, Ramanujam PS, Hvilsted S. 1998. Mean-field theory of photoinduced formation of surface reliefs in side-chain azobenzene polymers. Phys Rev Lett 80(1):89–92.

Pietsch U. 2002. X-ray and visible light scattering from light-induced polymer gratings. Phys Rev B 66(15):155430.

Pietsch U, Rochon P, Natansohn A. 2000. Formation of a buried lateral density grating in azobenzene polymer films. Adv Mater 12(15):1129–1132.

Ramanujam PS, Holme NCR, Hvilsted S. 1996. Atomic force and optical near-field microscopic investigations of polarization holographic gratings in a liquid crystalline azobenzene side-chain polyester. Appl Phys Lett 68(10):1329–1331.

Ramanujam PS, Pedersen M, Hvilsted S. 1999. Instant holography. Appl Phys Lett 74(21):3227–3229.

Rocha L, et al. 2001. Laser emission in periodically modulated polymer films. J Appl Phys 89(5):3067–3069.

Rochon P, Batalla E, Natansohn A. 1995. Optically induced surface gratings on azoaromatic polymer films. Appl Phys Lett 66(2):136–138.

Rochon P, Natansohn A, Callendar CL, Robitaille L. 1997. Guided mode resonance filters using polymer films. Appl Phys Lett 71(8):1008–1010.

Sanchez C, Alcala R, Hvilsted S, Ramanujam PS. 2000. Biphotonic holographic gratings in azobenzene polyesters: surface relief phenomena and polarization effects. Appl Phys Lett 77(10):1440–1442.

Saphiannikova M, Geue TM, Henneberg O, Morawetz K, Pietsch U. 2004a. Linear viscoelastic analysis of formation and relaxation of azobenzene polymer gratings. J Chem Phys 120(8):4039–4045.

Saphiannikova M, Henneberg O, Gene TM, Pietsch U, Rochon P. 2004b. Nonlinear effects during inscription of azobenzene surface relief gratings. J Phys Chem B 108(39):15084–15089.

Schaller RD, Saykally RJ, Shen YR, Lagugne-Labarthet F. 2003. Poled polymer thin-film gratings studied with far-field optical and second-harmonic near-field microscopy. Opt Lett 28(15):1296–1298.

Schmitt K, Benecke C, Schadt M. 1997. Pulsed, laser-induced holographic coupling gratings for waveguides made of cross-linkable polymers. Appl Opt 36(21):5078–5082.

Sharma L, Matsuoka T, Kimura T, Matsuda H. 2002. Investigation into the surface relief grating mechanism via XPS in new azobenzene based optical material. Polym Adv Technol 13(6):481–486.

Si JH, Qiu JR, Zhai JF, Shen YQ, Hirao K. 2002. Photoinduced permanent gratings inside bulk azodye-doped polymers by the coherent field of a femtosecond laser. Appl Phys Lett 80(3):359–361.

Srikhirin T, Laschitsch A, Neher D, Johannsmann D. 2000. Light-induced softening of azobenzene dye-doped polymer films probed with quartz crystal resonators. Appl Phys Lett 77(7):963–965.

Stiller B, et al. 2004. Optically induced mass transport studied by scanning near-field optical- and atomic force microscopy. Phys Low-Dimens Str 1–2:129–137.

Stockermans RJ, Rochon PL. 1999. Narrow-band resonant grating waveguide filters constructed with azobenzene polymers. Appl Opt 38(17):3714–3719.

Stracke A, Wendorff JH, Goldmann D, Janietz D, Stiller B. 2000. Gain effects in optical storage: thermal induction of a surface relief grating in a smectic liquid crystal. Adv Mater 12(4):282–285.

Sumaru K, Yamanaka T, Fukuda T, Matsuda H. 1999. Photoinduced surface relief gratings on azopolymer films: analysis by a fluid mechanics model. Appl Phys Lett 75(13):1878–1880.

Tabiryan N, Serak S, Dai XM, Bunning T. 2005. Polymer film with optically controlled form and actuation. Opt Express 13(19):7442–7448.

Tanchak OM, Barrett CJ. 2005. Light-induced reversible volume changes in thin films of azo polymers: the photomechanical effect. Macromolecules 38(25):10566–10570.

Tripathy SK, Viswanathan NK, Balasubramanian S, Kumar J. 2000. Holographic fabrication of polarization selective diffractive optical elements on azopolymer film. Polym Adv Technol 11(8–12):570–574.

Ubukata T, Seki T, Ichimura K. 2000. Surface relief gratings in host-guest supramolecular materials. Adv Mater 12(22):1675–1678.

Ubukata T, Seki T, Ichimura K. 2002. Surface relief grating in hybrid films composed of azobenzene polymer and liquid crystal molecule. Coll Surf A 198:113–117.

Viswanathan NK, Balasubramanian S, Li L, Kumar J, Tripathy SK. 1998. Surface-initiated mechanism for the formation of relief gratings on azo-polymer films. J Phys Chem B 102(31):6064–6070.

Viswanathan NK, Balasubramanian S, Li L, Tripathy SK, Kumar J. 1999a. A detailed investigation of the polarization-dependent surface-relief-grating formation process on azo polymer films. Jpn J Appl Phys 1 38(10):5928–5937.

Viswanathan NK, et al. 1999b. Surface relief structures on azo polymer films. J Mater Chem 9(9):1941–1955.

Wang X, Balasubramanian S, Kumar J, Tripathy SK, Li L. 1998. Azo chromophore-functionalized polyelectrolytes. 1. Synthesis, characterization, and photoprocessing. Chem Mater 10(6):1546–1553.

Watanabe O, et al. 2000. Transcription of near-field induced by photo-irradiation on a film of azo-containing urethane-urea copolymer. Mol Cryst Liq Cryst 345:629–634.

Wu YL, Natansohn A, Rochon P. 2001. Photoinduced birefringence and surface relief gratings in novel polyurethanes with azobenzene groups in the main chain. Macromolecules 34(22):7822–7828.

Yager KG, Barrett CJ. 2001. All-optical patterning of azo polymer films. Curr Opin Solid State Mater Sci 5(6):487–494.

Yager KG, Barrett CJ. 2004. Temperature modeling of laser-irradiated azo-polymer thin films. J Chem Phys 120(2):1089–1096.

Yager KG, Barrett CJ. 2006a. Novel photo-switching using azobenzene functional materials. J Photochemistry Photobiology A: Chemistry 182(3):250–261.

Yager KG, Barrett CJ. 2006b. Photomechanical surface patterning in azo-polymer materials. Macromolecules 39(26):9320–9326.

Yager KG, Barrett CJ. 2007. Confinement of surface patterning in azo-polymer thin films. J Chem Phys 126(9):094908–094908.

Yager KG, Tanchak OM, Barrett CJ, Watson MJ, Fritzsche H. 2006a. Temperature-controlled neutron reflectometry sample cell suitable for study of photoactive thin films. Rev Sci Instrum 77(4):045106-1–045106-6.

Yager KG, Tanchak OM, Godbout C, Fritzsche H, Barrett CJ. 2006b. Photomechanical effects in azo-polymers studied by neutron reflectometry. Macromol 39(26):9311–9319.

Yamaki S, Nakagawa M, Morino S, Ichimura K. 2000. Surface relief gratings generated by a photocrosslinkable polymer with styrylpyridine side chains. Appl Phys Lett 76(18):2520–2522.

Yang K, Yang SZ, Wang XG, Kumar J. 2004. Enhancing the inscription rate of surface relief gratings with an incoherent assisting light beam. Appl Phys Lett 84(22):4517–4519.

Yang K, Yang SZ, Kumar J. 2006. Formation mechanism of surface relief structures on amorphous azopolymer films. Phys Rev B 73(16).

Yang S, et al. 2002. Azobenzene-modified cellulose. Polymer News 27:368–372.

Yang SZ, Li L, Cholli AL, Kumar J, Tripathy SK. 2001. Photoinduced surface relief gratings on azocellulose films. J Macromol Sci Pure 38(12):1345–1354.

Yang SZ, Li L, Cholli AL, Kumar J, Tripathy SK. 2003. Ambenzene-modified poly (L-glutamic acid) (AZOPLGA): its conformational and photodynamic properties. Biomacromolecules 4(2):366–371.

Ye YH, Badilescu S, Truong VV, Rochon P, Natansohn A. 2001. Self-assembly of colloidal spheres on patterned substrates. Appl Phys Lett 79(6):872–874.

Yi DK, Kim MJ, Kim DY. 2002a. Surface relief grating induced colloidal crystal structures. Langmuir 18(6):2019–2023.

Yi DK, Seo E-M, Kim D-Y. 2002b. Fabrication of a mesoscale wire: sintering of a polymer colloid arrayed inside a one-dimensional groove pattern. Langmuir 18(13):5321–5323.

Yu Y, Nakano M, Ikeda T. 2003. Photomechanics: directed bending of a polymer film by light. Nature 425:145.

Yu YL, Nakano M, Maeda T, Kondo M, Ikeda T. 2005. Precisely direction-controllable bending of cross-linked liquid-crystalline polymer films by light. Mol Cryst Liq Cryst 436:1235–1244.

Zettsu N, Ubukata T, Seki T, Ichimura K. 2001. Soft crosslinkable azo polymer for rapid surface relief formation and persistent fixation. Adv Mater 13(22):1693–1697.

Zettsu N, Fukuda T, Matsuda H, Seki T. 2003. Unconventional polarization characteristic of rapid photoinduced material motion in liquid crystalline azobenzene polymer films. Appl Phys Lett 83(24):4960–4962.